Low Swelling Capacity of Highly Stretched Polystyrene Brushes

C. Devaux,[†] F. Cousin,[‡] E. Beyou,[†] and J.-P. Chapel*[,†,§]

Laboratoire des Matériaux Polymères et des Biomatériaux, UMR CNRS 5627, Université Claude Bernard Lyon 1, ISTIL, 43, Boulevard du 11 Novembre 1918, 69622 Villeurbanne Cedex, France, and Laboratoire Léon Brillouin, CEA-CNRS, CEA Saclay, 91191 Gif sur Yvette, France

Received December 7, 2004; Revised Manuscript Received March 9, 2005

ABSTRACT: We report the unusually low swelling capacity of highly stretched polystyrene chains grown on a silicon surface using "living" free radical polymerization. The control over the lateral density leads to brushes with a very high grafting density (up to >1.0 chain/nm^2). Neutron reflectivity measurements have evidenced two specific features of such brushes: (i) the controlled nature of the surface polymerization through a very homogeneous growth of homopolymer and copolymer chains; (ii) the highest volume fraction in good solvent $\Phi(z=0) = 0.85$ ever seen due to the highly stretched configuration of the dry chains, hindering a complete swelling of the layers and suggesting a significant deviation from predicted scaling laws.

Introduction

Polymer chains in confined geometry or in thin films are seen in a tremendous number of systems and devices of modern material science and technology. However, the behavior of such macromolecular chains near an interface is far from being understood. It deviates quite often from "bulk" properties with sometimes some contradictory results published on similar systems. The need for controlled (thickness, molecular weights, conformations, ...), stable (no dewetting or loss of material upon heating, ...), and reproducible thin films is then essential to go forward and try to understand what is really governing the dynamics in such constraint systems. Following this idea, we have developed an overall strategy to build up chemisorbed thin films with tunable architectures grown directly from silica surface through controlled macromolecular chemistry.[1] The process is split into two distinct steps: (i) Deposition of an initiator monolayer (triethoxysilane-terminated TEMPO) using the "reactive" Langmuir−Blodgett deposition technique. The control of the grafted initiator density (and therefore the chain grafting density σ) was shown to be efficient and highly reproducible. (ii) The nitroxide-mediated free radical polymerization of styrene, either hydrogenated (HS) or deuterated (DS). The main features of such kind of controlled process; i.e., the simultaneous growth of the chains and the fine-tuning of the lateral grafting density allow to build up brushes with different conformations from quite relaxed to very stretched chains, as illustrated in Figure 1 (see ref 1 for experimental details and polymer characteristics) through the plot of the brush thicknesses as a function of the PS molecular weight M_n (or alternatively the chain length N). For comparison purposes, similar PS chains were also grafted following the more classical onto approach, where an end-functionalized PS chains (triethoxysilane groups) were grafted directly onto the silica surface. The stretch S of the chain was estimated via the ratio measured thickness h/theoretical contour length of the chain L_0. In both grafting approaches (from and onto), the dry brush thickness h scaled linearly with the chain length N (M_n) and the lateral grafting density σ as expected in a bad solvent (air). But only the from approach combined with the LB deposition technique gave us access to the regime of very dense brushes with a stretch (S) between 0.7 and 0.9 and grafting density above 1 chains/nm^2, as clearly evidenced in the dense regime part of Figure 1.

Furthermore, besides the control over the thickness, the stretch, and the polydispersity (IP 1.1), the potentially active chain ends offer the unique advantage to reinitiate the polymerization and to create through successive runs a multilayer structure with controlled characteristics, as illustrated in Figure 2.

In the past, scaling laws have been verified in different cases for neutral brushes with moderate lateral density[2−4] (when charged, polymer brushes follow a different scaling behavior[5]). In a poor solvent, the thickness h scales linearly with either the chain length N or the grafting density σ ($h \propto N\sigma$). In a good solvent, the chains adopt a more extended conformation consecutive to the solvent−polymer interactions determined by a balance between the interactions that promote stretching and the associated loss of chain conformational entropy [6] (h/N scales with $\sigma^{1/3}$).[7] In that case, however, the brush becoming a continuous layer of solvated chains, the thickness is indeed difficult to ascertain. Neutron reflectivity measurements are then perfectly appropriated to study the influence of solvent on polymer chains at interface:[8,9] the polymer density profile depends strongly on the brush structures[10−12] (Figure 2).

In this paper we report the peculiar low swelling capacity of highly stretched PS chains in good solvent. The combined influence of very high lateral density (up to >1.0 chain/nm^2) and chain length N on brush structures will be investigated experimentally in both dry and swollen states. Moreover, the roughness of either polymer/solvent or polymer/polymer (HPS/DPS layers) interfaces can also be probed using neutron reflectivity measurements. A low roughness value of the polymer/polymer interface will certainly ascertain both

[†] Université Claude Bernard Lyon 1.
[‡] CEA-CNRS.
[§] Now at Complex Fluid Laboratory, UMR CNRS/Rhodia Inc., Cranbury−Princeton, NJ.
* Corresponding author. E-mail jeanpaul.chapel@us.rhodia.com or jchapel@princeton.edu.

10.1021/ma047478y CCC: $30.25
Published on Web 04/05/2005

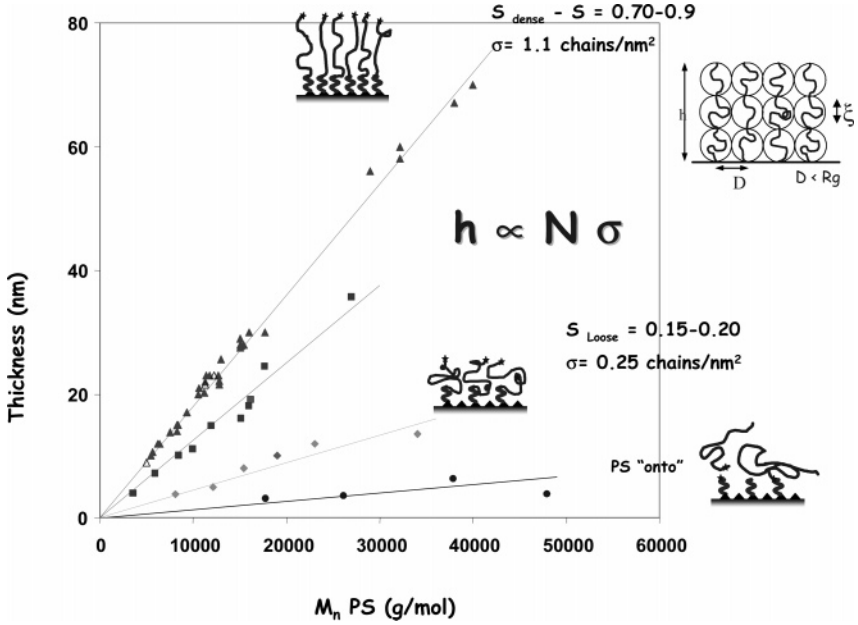

Figure 1. Brush thickness measured by ellipsometry in air as a function of the molecular weight M_n (or chain length N) of PS chains either grafted from or onto the silica surface. For a given molecular weight, the from approach (combined with the LB deposition technique that imposes the lateral density) is incomparably more efficient to produce thick and then dense layers than the regular onto approach.

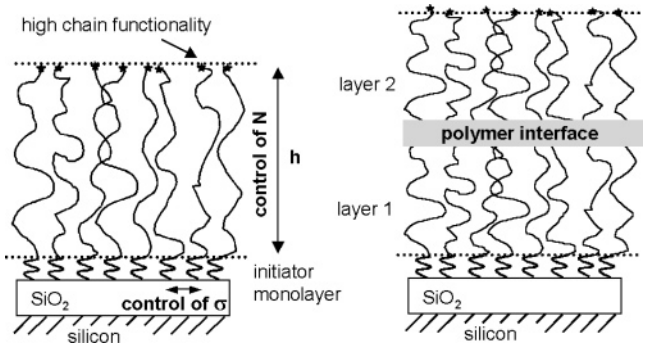

Figure 2. Schematic view of the different structures accessible using our approach through an accurate control of the grafting density and the molecular weights. Because of the controlled nature of the polymerization, reinitiation of the polymerization in successive runs enables also to tailor multilayer with controlled features.

the simultaneous growth of the chains through the controlled TEMPO-like polymerization and the efficiency of the reinitiation process that permits multilayer tailoring.

Materials and Methods

Neutron Reflectivity Experiments. The neutron reflectivity measurements were performed on the time-of-flight reflectometer EROS at LLB. Two geometries were used. In the first one the silicon/air interface is probed with a q range varying from 0.008 and 0.07 Å^{-1}. In the second one, the silicon/deuterated toluene interface is probed (the neutron getting through the sample) with a q range varying from 0.01 to 0.08 Å^{-1}. A specific homemade cell was used to perform the swelling experiments in d-toluene (Figure 3). During the experiment, we use all the wavelengths λ provided by the neutron source from 3 to 25 Å with a constant $\Delta\lambda$ of 0.3 Å. We use for the silicon/air interface $\theta = 0.93°$ and for the silicon/deuterated toluene $\theta = 1.23°$ with a $\Delta\theta$ of 0.05°. The experimental resolution is taken into account in the fitting procedure.

Sample Features. The brush preparation and characterization were achieved according to methods previously reported.[1] The hydrogenated polystyrene brush (HPS) features

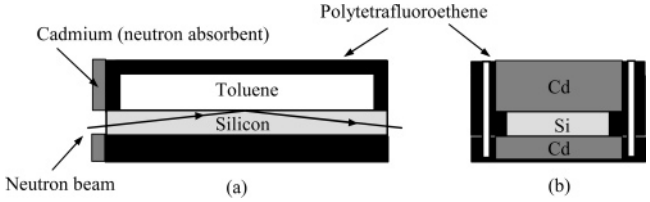

Figure 3. Schematic view of the homemade cell used in swelling experiment: (a) longitudinal view; (b) face view. It is made of two blocks of PTFE. In the upper part a reservoir for the toluene and a volume corresponding to the silicon wafer are removed. A neutron absorbent is fixed to the cell, protecting the PTFE parts, to avoid incoherent scattering from PTFE.

Table 1. Features of the Three Hydrogenated Polystyrene Brushes[a]

sample	N	h (Å)	L_0 (Å)	σ (chain/nm^2)	h/L_0
A	120	100	300	0.55	0.35
B	120	200	300	1.10	0.70
C	270	470	680	1.05	0.70

[a] N is the average monomer content of the grafted chain (estimated by SEC), and h is the brush thickness measured in air by spectroscopic ellipsometry (ES4G from SOPRA). L_0 corresponds to the theoretical extended contour length calculated with a repeating unit of 2.6 Å. σ is computed using the following equation: $\sigma = N_A h\rho/M_n$. M_n (= $104N$) is the polymer molecular weight, N_A is the Avogadro number, and $\rho = 1.05$ g/cm^3 is the classical bulk polystyrene density.

are given in Table 1. The brush thicknesses were obtained in air (dry state) through ellipsometric measurements with a 15−20 Å layer of native silica and a 10−15 Å layer of grafted initiator.

Samples A and B have a different grafting density: σ_B is twice σ_A with the same chain length ($N_A = N_B$). Samples B and C have a different chain length: $N_C \sim 2N_B$ with the same grafting density $\sigma_C = \sigma_B$. In both case, the grafting density being quite high (0.5 and 1.0 chain/nm^2, respectively), the chains are then already extended in air. The stretch of the chain is estimated via the ratio measured thickness h/theoretical contour length of the chain L_0. The dry brush thickness h scales linearly with chain length N and lateral grafting density σ as expected in a bad solvent (air).

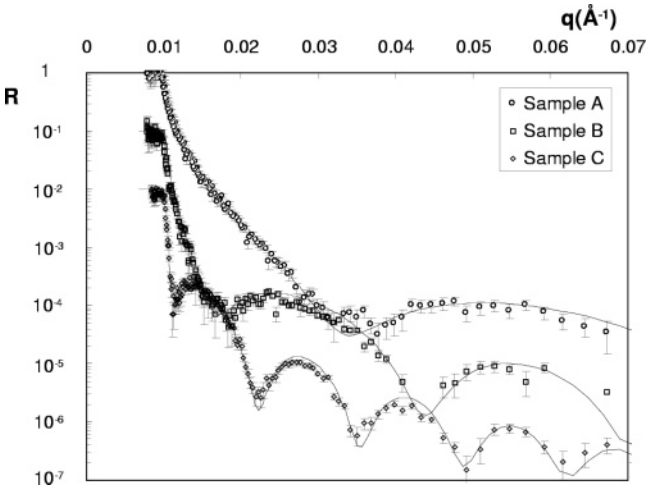

Figure 4. Experimental reflected curves and corresponding fits for the three hydrogenated brushes. Intensities of curves for samples B and C are respectively magnified by a factor 0.1 and 0.01 for better reading.

Table 2. Neutron Reflectivity Results[a]

sample	h' (Å)	h_s (Å)	$h_{\Phi=0}$ (Å)	$\Phi(z=0)$	h_s/L_0	h_s/h'	SR
A	110	190	300	0.60	0.60	1.7	0.40
B	220	270	300	0.85	0.90	1.2	0.20

[a] For sample C, $h' = 460$ Å, h' is the dry thickness measured by neutron reflectivity. h_s corresponds to the swollen brush thickness. $h_{\Phi=0}$ is the thickness value at the end of volume fraction Φ vs distance (z) profile. $\Phi(z=0)$ is the volume fraction of polymer at surface ($z = 0$). SR is the swelling ratio calculated from the defined relation.

Results and Discussion

Dry Brushes. The reflectivity curves measured on each sample are presented in Figure 4. All curves have been fitted by model reflectivity curves calculated by the standard optical matrix method. Best fits between the calculated and experimental spectra were obtained by minimizing least-squares χ^2. A three-layer model was used that includes the SiO_2 layer at the surface of silicon with a neutron density length N_b of 3.41×10^{-6} Å^{-2}, the initiator layer mainly constituted of alkyl chains with a N_b close to 0 and the PSH layer with a N_b of 1.41×10^{-6} Å^{-2} (Table 1).

The sizes of both the SiO_2 layer (15−20 Å) and the initiator layer (5−10 Å) were kept constant, and their values were previously determined in a series of experiments performed on pure PSD grafted brushes on the basis of the ellipsometric measurements. The large neutronic contrast between the PSD ($N_b = 6.3 \times 10^{-6}$ Å^{-2}) and the others layers (N_b of Si is 2.07×10^{-6} Å^{-2}) allows an accurate determination of these different layers at the surface. Fits have been realized with a zero roughness at the air/layer interface and with a polymeric volume fraction Φ of 1 (Figure 4).

Results are gathered in Table 2. It should be noted that both ellipsometric (h) and neutron reflectivity (h') thickness measurements agree within 10%. The specific features of dry brushes are here clearly evidenced: (i) for a given chain length N (or molecular weight) and a doubled grafting density, the measured thickness h'_B is twice h'_A; (ii) for a given grafting density, the thickness h' is proportional to chain length N (samples B and C).

Homogeneity of the Brushes during Polymerization Growth. Prior to the determination of the structure of the swollen brushes, we have checked the homogeneity of the dry brushes. Taking profit from high neutronic contrast between DPS and HPS, we have specifically designed a DPS/HPS copolymer brush to check a posteriori the homogeneity of the chain growth front during the polymerization from the surface (sample D).

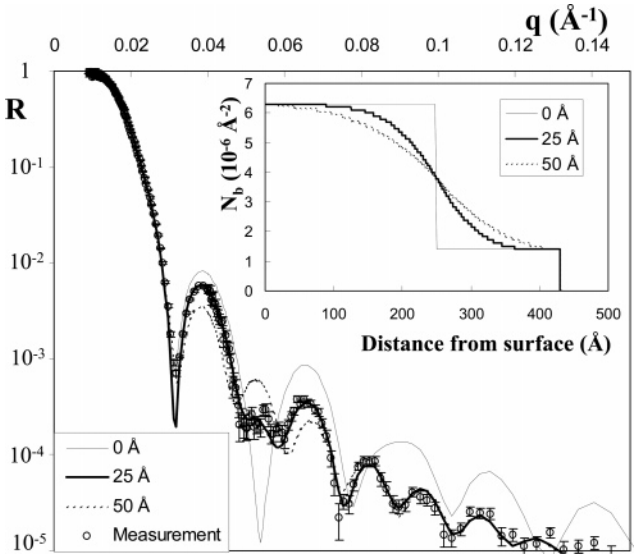

Figure 5. Reflectivity curves of a dry HPS−DPS copolymer brush (sample D) and resulting fits with different interdiffusion layers. Widths are given in the caption. Corresponding neutron density profiles are shown in the inset.

Though the polymer chains behave finally as a single physical unit, its ability to scatter neutrons keeps the memory of its synthesis. Homogeneity of the copolymer brush during the growth is linked to the width of the interdiffusion layer of the DPS/HPS interface. The latter can indeed be accurately determined by neutron reflectivity. The bilayer was built up from two polymerization runs in a row: a first one with deuterated styrene ($N = 95$) followed by a second one with hydrogenated styrene ($N = 90$). The DPS and (DPS + HPS) dry thicknesses obtained by ellipsometric measurements were respectively 230 and 420 Å. Neutron reflectivity measurements were carried out in the dry state (Figure 5).

There are irregular Kiessig fringes arising from the three-layer structure (HPS, DPS, and the total PS layer). It is fitted by a four-layer model including the SiO_2 layer (15 Å), the initiator layer (5 Å), the PSH layer, and the PSD deuterated layer. Best fits are obtained with a PSH and a PSD layer of 250 and 180 Å, respectively, with an interdiffusion layer of 25 Å. The latter, with an extension of $2\sigma_{int}$, is taken into account in the calculation of the theoretical reflectivity patterns by replacing the discrete interface of N_b between PSH and PSD layers by an error function of full half-width height σ_{int}. It is equivalent to multiply the reflectivity curve by a Debye−Waller term DW: $DW = \exp(-4q_H q_D \sigma^2_{int})$, where q_H and q_D are defined by $q_H^2 = q^2 - 4\pi N_b$ (PSH) and $q_D^2 = q^2 - 4\pi N_b$ (PSD), respectively.

Large oscillations, due to small layers, progressively vanish when increasing the interdiffusion layers as HPS and DPS are not anymore precisely defined; only the small oscillations due to the large layer remain. The progressive apparition or disappearance of the fringes enables to get unambiguously σ_{int}.

The value of 25 Å for σ_{int}, on a total layer of 430 Å, underlines the homogeneity of the brush growth and the

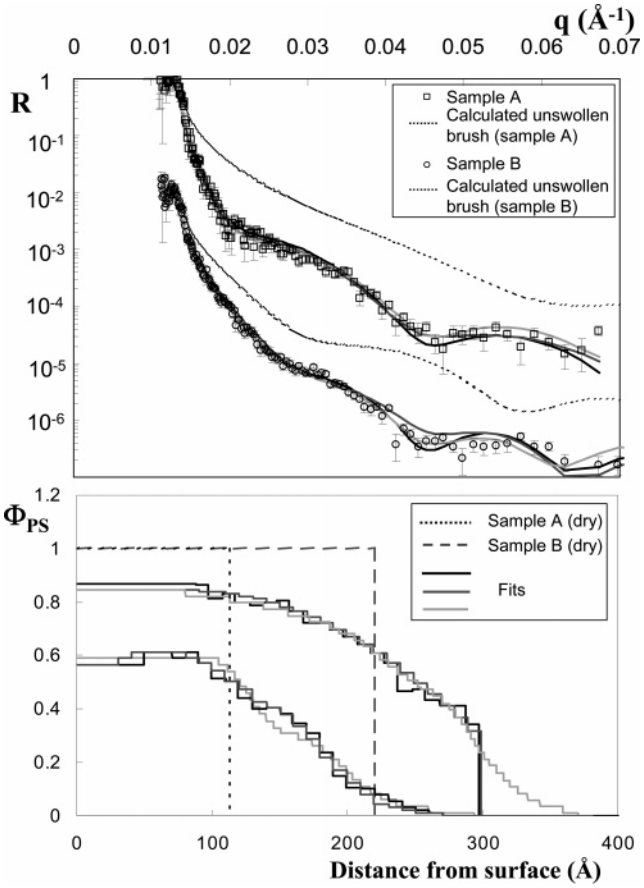

Figure 6. Experimental reflected curves and corresponding fits for the two different HPS brushes A and B. Corresponding fits, calculated curves for unswollen brushes, and volume fraction profiles are also indicated. Intensity of curve corresponding to sample B is magnified by a factor 0.01 for better reading.

possibility to form multilayer with well-defined interfaces.

Both the controlled initiator layer deposition and the controlled nature of the polymerization enable efficiently to build very dense brushes with distinct copolymer structures. It should be emphasized that brush structure does not depend on the chain length N but exclusively on the grafting density σ.

Swollen Brushes. Though the brush structure does not depend on N, we have studied the effect of lateral grafting density on swollen HPS brushes features (samples A and B) in good solvent. Deuterated toluene has been chosen for solvent because it offers a good neutronic contrast to PSH. The results are reported in Figure 6 and Table 2. The reflected curves are compared to the calculated ones obtained for the unswollen brushes A and B in the same experimental conditions, i.e., if deuterated toluene would have been a poor solvent for HPS.

The experimental reflected intensity appears weaker than in the unswollen case due to the decrease of the polymer/solvent contrast, indicating "partially" swelled brushes. The Kiessig fringes are still visible but less marked in the presence of the solvent. The polymer layer has hence finite size with a less defined polymer/solvent interface: the density profiles are no longer steplike. For both samples, the Kiessig fringes are shifted toward lower q, and the values of their minima are located at the same q. The solvent has thus enlarged the thickness of the layers, which are for both sample roughly the same even though the dry thickness of B was twice the A one. Reflected curves have been fitted again by a three-layer model: SiO_2 layer (15 Å), the initiator layer (5 Å), and a continuous profile of swelled chains which ensures polymer conservation from dry to swollen state (divided in layers of 10 Å). Both the experimental resolution and the lack of phase information do not guarantee a unique profile from the fitting procedure. Nevertheless, both the conservation of the dry polymeric mass and the maximal extension of the swollen brushes (minima of Kiessig fringes) allow getting a series of close profiles that fit experimental curves within error bars. Three calculated profiles are presented for each sample. For sample A, it has not been possible to fit the data with a profile having a parabolic tail.

Results of Table 2 are averaged on the three calculated profiles. The measured swollen brush thickness h_s are computed from the Φ vs z profile as an effective layer containing 95% of the polymer. It should be pointed out that the thickness for which Φ reaches 0 is the same for samples A and B ($\propto$ 300 Å). Indeed, from such low polydispersity index ($\sim$1.1), one can infer that less than 10% of the chains with a higher molecular weight (than the average M_n) are not fully extended. A higher fraction of such chains would have killed any oscillation in the reflectivity curves (Figure 4). This thickness corresponds then nearly to the fully extended PS chain (L_0) of most of the chains. Obviously, these results will not be valid for highly (above 1.3) polydispersed chains.[12]

From the profile in Figure 6, the volume fraction Φ at the surface ($z = 0$) keeps for the highest grafting density the unusual value of 0.85, to our knowledge the highest value ever reported in the literature. This value is an indirect illustration of the stretched conformation of the chains in the dry state. In that case the solvent has some difficulty to penetrate the layer leading to a somehow low swelling capacity. The latter rate seems to be mainly dependent on the lateral grafting density of the brushes. We can then define the degree of swelling as the ratio h_s/h' or from the following relation:

$$\mathrm{SR} = 1 - \frac{\int_0^{h'} \phi(z)\,\mathrm{d}z}{\int_0^{h'} \mathrm{d}z}$$

It turns out that the solvent incorporation is notably reduced when increasing σ. Results, reported in Table 2, indicate an effective decrease of the swelling ratio with the lateral grafting density h_s/h' and SR decrease with σ as expected,[5,14,15] but with much lower values (1.7 and 1.2) reflecting very dense brushes. Considering such very low swelling capacity, it is interesting to compare the experimental results to scaling law predictions. Depending on the grafting density two limiting regimes are achievable: for low or moderate densities ($\sigma < 0.2$ chain/nm^2), h_s/N scales with $\sigma^{1/3}$. When the grafting density approaches the highest coverage limit, where *all* the chains are by definition fully stretched, the thickness h_s should not depend anymore on the grafting density, h_s/N being constant and $\sim\sigma_{\max}^{1}$. In between, the density exponent should likely vary continuously from $^1/_3$ to 1.

In the case of our real dense brushes, $h_s/N \propto \sigma^n$ with $n = 0.5$. The similarity between this value and the $n =$

$^1/_2$ obtained for moderately grafted brushes in Θ conditions[15−17] is likely a pure coincidence. Beyond the few samples investigated here, further work is then needed in the high-density regime to accurately get reliable scaling law exponents.

The differences seen in this study are then related to the very high grafting density which reduces the brush swelling capacity in good solvent (toluene is a good solvent of PS at room temperature).

The stretch of the chains estimated via h/L_0 (dry state) and h'/L_0 (swollen state) increases through swelling from 0.35 to 0.6 and from 0.7 to 0.9 for samples A and B, respectively. At such densities chains have nearly an extended conformation, and the probability of a monomer−monomer interaction is nearly 6 times higher ((85/100)/(15/100)) than a toluene−monomer interaction (styrene and toluene have similar molar volumes).

Conclusion

The neutron reflectivity measurements presented in this paper have clearly evidenced the perfect control over the final properties of PS brushes grown from silica surface through the thin film processing described in ref 1. The very homogeneous growth of the chains leads to homogeneous brushes with stretch or conformations controlled exclusively by the grafting density σ and thicknesses tunable independently through the (controlled) chain molecular weights. In the case of very dense brushes (>1.0 chain/nm^2) in good solvent, the highest volume fraction (0.85) ever measured for polymer chains leads to a significant reduction of the swelling capacity of the layer and a noticeable deviation from classical brush scaling laws—a result somehow not completely surprising for such high volume fractions where scaling laws, applicable to semidilute polymer brushes in good solvent, have no reason to hold anymore.

Acknowledgment. We acknowledge A. Menelle for fruitful discussions and the reviewers for their pertinent comments and suggestions that helped us to improve our manuscript.

References and Notes

(1) Devaux, C.; Beyou, E.; Chaumont, Ph.; Chapel, J. P. *Eur. Phys. J. E* **2002**, *7*, 345. Devaux, C.; Chapel, J. P. *Eur. Phys. J. E* **2003**, *10*, 77.
(2) Alexander, S. *J. Phys. (Paris)* **1977**, *38*, 983.
(3) De Gennes, P. G. *Macromolecules* **1980**, *13*, 1069.
(4) Halperin, A.; Tirrell, M.; Lodge, T. P. *Adv. Polym. Sci.* **1992**, *31*, 100.
(5) Biesalski, M.; Ruhe, J. *Macromolecules* **2002**, *35*, 499. Biesalki, M.; Rühe, J. *Macromolecules* **2003**, *36*, 1222.
(6) Brown, H. R.; Char, K.; Delin, V. R. *Macromolecules* **1990**, *23*, 3385.
(7) Auroy, P.; Auvray, L.; Léger, L. *Phys. Rev. Lett.* **1991**, *66*, 719.
(8) Field, J. B.; Toprakcioglu, C.; Ball, R. C.; Stanley, H. B.; Dai, L.; Barford, W.; Penfold, J.; Smith, G.; Hamilton, W. *Macromolecules* **1992**, *25*, 434.
(9) Lee, L. T.; Jean, B.; Menelle, A. *Langmuir* **1999**, *15*, 3267−3272.
(10) Marzolin, C.; Auroy, P.; Deruelle, M.; Folkers, J. P.; Léger, L.; Menelle, A. *Macromolecules* **2001**, *34*, 8694.
(11) Grest, G. S.; Murat, M. *Macromolecules* **1993**, *26*, 3108.
(12) Milner, S. T.; Witten, T. A.; Cates, M. E. *Macromolecules* **1988**, *21*, 2610.
(13) Milner, S. T.; Witten, T. A.; Cates, M. E. *Macromolecules* **1989**, *22*, 853.
(14) Yamamoto, S.; Ejaz, M.; Tsujii, Y.; Matsumoto, M.; Fukuda, K. *Macromolecules* **2000**, *33*, 5602. Yamamoto, S.; Ejaz, M.; Tsujii, Y.; Matsumoto, M.; Fukuda, K. *Macromolecules* **2000**, *33*, 5608.
(15) Sirard, S.; Gupta, R.; Russell, T. P.; Watkins, J.; Grenn, P.; Johnston, K. P. *Macromolecules* **2003**, *36*, 3365.
(16) Karim, A.; Satija, S. K.; Douglas, J. F.; Ankner, J. F.; Fetters, L. J. *Phys. Rev. Lett.* **1994**, *73*, 3407.
(17) Kilbey, S. M., II; Watanabe, H.; Tirrell, M. *Macromolecules* **2000**, *34*, 5249.

MA047478Y